applied sciences

MDPI

Article

Numerical Investigations of Pile Group Foundations under Different Pile Length Conditions

Chuheng Zhong [1,2], Ze Chen [1] and Jinzhi Zhou [1,*]

[1] School of Civil Engineering, Architecture and Environment, Hubei University of Technology, Wuhan 430068, China; zhongchuheng@gmail.com (C.Z.); chenze0015@gmail.com (Z.C.)
[2] Key Laboratory of Health Intelligent Perception and Ecological Restoration of River and Lake, Ministry of Education, Hubei University of Technology, Wuhan 430068, China
* Correspondence: zhoujinzhi@hbut.edu.cn

Abstract: At present, group pile foundations with the same length of pile base are used basically in large-scale slope group pile foundation projects. Therefore, pile group foundations with piles of different lengths have a certain research value. Based on the actual working condition of a bridge group pile foundation, a similar model is established, which is imported into the FLAC3D 6.0 finite element software package together with the processed relevant data, and the bearing performance of the cap-group pile foundation under the joint action of axial uniform load and landslide thrust is studied. The study shows: under the same bearing conditions, the settlements of group pile foundations with the same pile length and different pile lengths are similar, and the settlements of the rear row of piles is significantly higher than those of the front row of piles; the settlement of the cap platform in the area without backfill soil is different from that in the area with backfill; the front row of piles has some negative displacement within the range of 10 m below the equivalent sliding surface, and the displacement of the pile body from the back row of piles to the front row of piles increases linearly; the maximum bending moment of the foundation pile is at the position of the gravel soil layer, and as the load changes, the position of the maximum bending moment point will also change; the plastic zone of the uppermost gravel soil layer in the slope model has the tendency of penetration, but it is truncated by the group of piles, and the factor of safety is 2.4 in the case of 100 KN axial uniform load, this structure tends to be stabilized, and the factor of safety decreases with the increase in the load. The analysis of the bearing characteristics of group piles under horizontal and vertical loads and its related conclusions can be used as a reference for related engineering design.

Keywords: group pile; numerical simulation; displacement; bending moment

Citation: Zhong, C.; Chen, Z.; Zhou, J. Numerical Investigations of Pile Group Foundations under Different Pile Length Conditions. *Appl. Sci.* **2024**, *14*, 1908. https://doi.org/10.3390/app14051908

Academic Editor: Cheng-Yu Ku

Received: 6 January 2024
Revised: 13 February 2024
Accepted: 22 February 2024
Published: 26 February 2024

1. Introduction

Pile foundations are widely used in various infrastructure engineering fields due to their numerous advantages, including high vertical bearing capacity, stability, and adaptability to different site conditions. In many building foundations, the pile group-cap system is commonly adopted, where both the piles and the cap work together to support the loads from the superstructure and soil deformation. In the southwest region of China, where railroad lines often need to cross steep slopes and deep valleys, a considerable number of bridge group pile foundations are constructed. However, the challenging terrain, geological conditions, and alignment selection in these areas increase the risk of landslides caused by factors such as heavy rain, earthquakes, and human activities. These landslides can result in soil deformation and overall sliding, endangering the safety of the bridge structure. Therefore, it is crucial to fully consider the stability of the group pile foundation under the influence of the slope when constructing such foundations.

Numerous scholars have conducted in-depth analyses and studies on group pile foundations on steep slopes, with a significant focus on studying group piles under vertical loads [1–5]. For instance, M. Bharathi [6] found that changing the load direction can significantly reduce the peak displacement of the pile group. B. B. Sheil [7] established a database of simplified models to predict the non-linear pile interaction within vertically loaded pile groups. S. Carbonari [8] evaluated the effects of pile geometry and inclination on soil-structure interaction. X.-y. Bian [9] proposed a method for evaluating the reliability of pile foundations in limit states.

When it comes to physical tests, model tests are often preferred as they can more accurately simulate real field environments. Y. Zhang [10], through quasi-static tests on specific group pile foundation models, revealed that the ultimate lateral force of the pile group is not solely determined by the yielding force of individual piles. K. Chaikla [11] characterized the bearing capacities and deformation behavior of inclined pile foundations subjected to vertical and horizontal loads in pile-modeled tests. F. Liang [12] reported results from multiple shaking table tests, focusing on the transverse response of pile group foundations. Z. Chen [13] conducted shaking table tests, which indicated that the inclusion of a drainage structure significantly improved the stability and safety of the bridge system. G. Fiorentino [14] studied the interaction effects between a scaled bridge model, abutments, foundation piles, and backfill soil. M. Sharafkhah [15], through physical model tests, indicated that the ultimate bearing capacity of the piled raft foundation is considerably higher than that of a free-standing pile group with the same number of piles.

Numerical simulation is a highly effective approach for conducting comparative analyses under different working conditions and parameter situations, compensating for the limitations of physical model testing methods. Among various numerical simulation methods, finite element analysis stands out as it can overcome the constraints of irregular slope geometries and material inhomogeneity. It offers a rigorous theoretical foundation and calculation results that fully satisfy static permits, strain coordination, and stress–strain ontological relationships. Consequently, this method is widely applied in analyzing various complex and large-scale engineering scenarios. For example, B. Ukritchon [16] investigated the distribution of pile forces in a group pile foundation under vertical loads and large moments using numerical simulation methods. D. Kong [17] confirmed through numerical simulations that pile foundations with high-rise pile caps can better resist seismic loads than those with low-rise pile caps. L. Qu [18] conducted three-dimensional finite element simulations to examine the effects of sloping ground on the vertical pile-to-pile interaction for end-bearing piles embedded in homogeneous soil. M. R. Kahyaoglu [19] utilized numerical simulations to study the influence of pile groups on soil arches. J. Lian [20] analyzed bucket foundations and group piles using the ABAQUS 2020 software. Kavvadas, M [21] proposed an MSS constitutive model for structured soils and analyzed the advantages of this model. Savvides, A. A. [22] used a modified Cam-Clay failure criterion to analyze the distribution of failure load and displacements in different soil depths.

This article presents the depiction of the slope's basic appearance based on actual topographic maps. A model is established and imported into the FLAC3D numerical simulation software for calculation. In this particular group pile foundation project, the foundation piles are relatively long and penetrate deep into the rock. Additionally, the bottom rock layer has a strong embedding capacity. To meet the basic stability requirements of the group pile foundation while conducting numerical simulations, the author reduces the length of the foundation piles based on the load conditions. This approach provides an effective piling scenario and enhances the economic efficiency of the project.

2. Bearing Principle

Steep slope group pile foundations, often situated on steep slopes or riverbanks, exhibit distinct bearing mechanisms and deformation characteristics compared to common group pile foundations on flat ground. These characteristics include the steep slope effect on the loaded section and the embedding depth effect on the embedded section. Many scholars use the classic Broms theory of lateral strength of piles to assess the bearing capacity of piles under lateral loads. This theory is simple and practical, requiring only simple parameters, making it suitable as a preliminary assessment tool. However, this theory is only applicable to small lateral displacements and relatively small lateral loads. Therefore, for the case of group pile bearing capacity discussed in this article, this theory does not apply.

The stress situation is depicted in Figure 1. In Figure 1, the distance b1, from the plane of point O to the slope surface at the front side of the foundation, should not be less than 4d, where d represents the diameter of the pile. The value of 4d corresponds to four times the diameter of the pile. If b1 is less than 4d, the analysis plane at point O should be lowered by d1, ensuring that b1 is not less than 4d. By doing so, the bearing performance of the soil between the piles and the soil on the front side of the foundation within this range is not considered. The soil behind the foundation within this depth should act in the form of active earth pressure q′ on the pile foundation. In the loaded section above the sliding surface, the pile body primarily experiences landslide thrust. Conversely, in the embedded section below the sliding surface, the pile body mainly encounters the foundation reaction force. The foundation reaction force increases as the piles get closer to the front slope face. Consequently, with the same length of each foundation pile, the back row of piles with excessive bearing performance can be made shorter. However, the length difference of the group pile foundation should not be too significant. Therefore, the pile length can be adjusted appropriately according to the slope conditions.

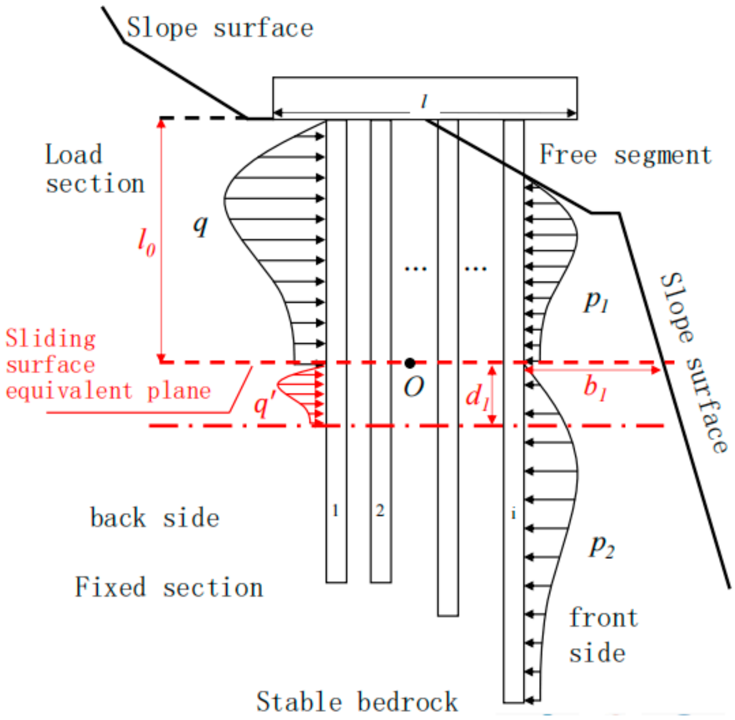

Figure 1. Pile load arrangement.

3. Model Building

To investigate the stability of a group pile foundation with varying pile lengths in multiple strata, the FLAC3D simulation and calculation software is utilized to simulate the corresponding model. FLAC3D is capable of three-dimensional modeling and analysis, supports multi-physics coupling, utilizes multi-core processors and cluster computing systems for parallel computing, and has powerful post-processing capabilities. However, FLAC3D has limited modeling capabilities and requires the assistance of external tools. Rhino 7 (a 3D modeling software package known for its powerful modeling capabilities and flexibility, Rhino's NURBSD modeling technology accurately describes surfaces and curves, enabling users to create high-quality geometric models) can draw a slope model according to the actual project, Griddle (a built-in plugin in Rhino that allows more refined meshing), and HyperMesh 2019 (professional finite element pre-processing software that provides powerful tools for the creation and preparation of finite element models; it supports various meshing techniques, including automatic and manual meshing, ensuring the accuracy and efficiency of numerical simulations) can generate a grid according to the model. The official websites of all software are displayed in Appendix A. The generation of grids using Rhino with Griddle may result in errors and mesh tearing; therefore, using Rhino with HyperMesh is a more suitable choice, ensuring a more coherent and aesthetically pleasing grid. The slope model is initially created using Rhino and exported as a STEP format file. This exported model file is then imported into HyperMesh for grid generation. The mesh type selected is Tetra (the type of grid is triangular), with a minimum size of 0.5 m and a maximum size of 3 m. After the necessary processing, the input format file can be opened within the Grid option of FLAC3D.

The dimensions of the slope model are 48 m × 239.5 m × 400 m, with an average slope of 25.9°. In this model, the X direction represents the 48 m length, with point O situated at the middle of this shorter side. The Y direction corresponds to the 400 m length of the model, and the Z direction represents the height of the model, measuring 239.5 m. The two side faces perpendicular to the X-axis constrain the X-direction displacement, while the two side faces perpendicular to the Y-axis constrain the Y-direction displacement. The bottom face constrains the Z-direction displacement. The model consists of three different soil layers, namely gravel soil, strongly weathered sandstone, and weakly weathered sandstone. The average slope of the gravel soil layer is 26.4° while the average slopes of the strongly weathered sandstone layer and the weakly weathered sandstone layer are 31.4° and 30.9°, respectively. The main mechanical parameters of the rock layers in the slope are presented in Table 1.

Table 1. Parameters of different soil layers.

Soil Layer	Bulk/(MPa)	Shear/(MPa)	Cohesion/(KPa)	Friction/(°)	Poisson's Ratio
gravel soil	59.03	12.4	14.5	22	0.40
strongly weathered sandstone	335.04	109.64	180	45	0.36
weakly weathered sandstone	169.6	320	32	53	0.34

The slope-cap-group piles in this study are modeled using an elastic model, known for their fast computation speed. This model provides a simplified representation of stress and deformation behaviors in the grid and helps identify areas of stress concentration. It requires two parameters, bulk modulus, and shear modulus, and quickly achieves an initial stress balance in the ground. Once the initial stress balance is achieved, the gravel soil layer is excavated, and group piles are installed. Each foundation pile extends through the gravel soil layer and the highly weathered rock layer until reaching the weakly weathered rock layer, which acts as the holding layer. The group piles are arranged in a 9 × 8 layout, with 9 rows perpendicular to the loading direction and 8 rows parallel to it. The spacing between piles is 3 m, and the diameter of the foundation piles is set at 3 m. The length of each row of foundation piles varies from 54 m to 70 m, as follows: 54 m, 58 m, 60 m, 62 m, 64 m, 66 m, 68 m, 70 m. The resulting model is shown in Figure 2. Different colors represent different groups. For this study, the middle row of foundation piles is chosen, and they are numbered 1 to 9 based on their order from shortest to longest. The foundation piles used in the model are C30 concrete piles. After setting up the group piles, a cap is placed on top of them, subjecting it to a uniform load of 100 kN. To improve the accuracy of the results, a control model is also created. In this control model, all foundation piles are set to a length of 70 m while maintaining other parameters consistent with the previous model. For convenience and adherence to international convention, the row of piles closest to the slope is referred to as the front pile row, the row away from the slope is called the rear pile row, and the row located in the middle of the front and rear pile rows is called the middle pile row. This naming convention is used for the sake of convenience and adherence to international standards.

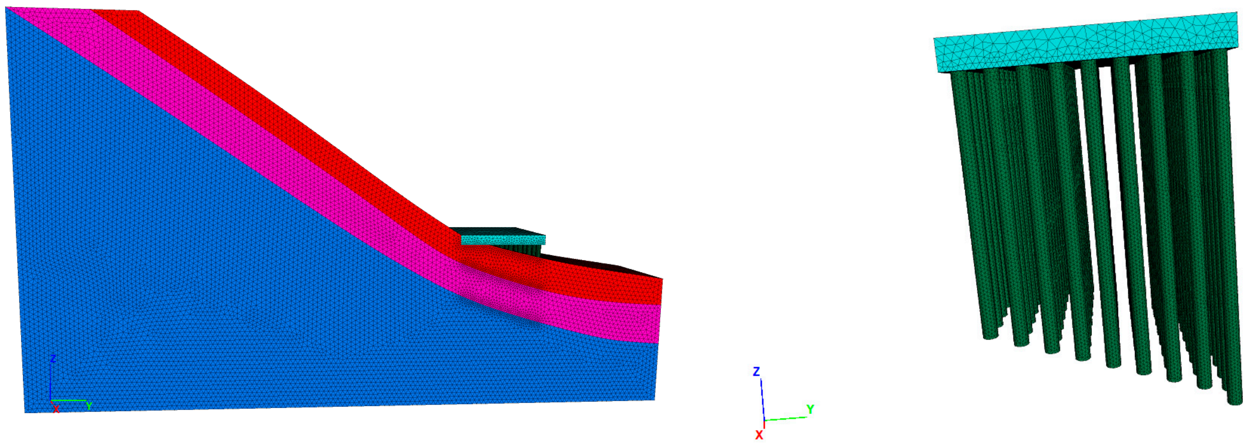

(**a**) (**b**)

Figure 2. (**a**) the slope model; (**b**) the pile model.

After setting up the slope-cap-group pile system, it is important to define the contact surfaces. Contact surfaces play a crucial role in the simulation process, especially between different materials. As the pile group undergoes stress loading, shear forces and relative displacement occur between the soil body and the cap. The contact surfaces enable the analysis of sliding, separation, and closure on these interfaces under specific loading conditions.

The entire calculation process proceeds as follows: Firstly, the initial stress field generated by the self-weight of the soil body is computed as a priority. This initial stress field is then saved after achieving stress balance. Next, the gravel soil layer is excavated, and appropriate values are assigned to the cap and foundation of the group piles. Contact surfaces between the group piles and each soil layer are established. Finally, a static vertically distributed load is applied to the cap until the entire model reaches equilibrium. The resultant stress field is saved, and finite element post-processing is conducted for further analysis.

To sum up, the steps of using FLAC3D for finite element simulation of the pile group foundation are as follows: Based on the actual geometry and size of the slope and pile group, create the corresponding three-dimensional finite element mesh, and import the model into FLAC3D. Define the material properties of the soil layers and assign properties to the mesh elements Bulk, Shear, Cohesion, and Friction. Apply boundary conditions by constraining the displacements at the bottom and surrounding areas of the model, while allowing displacements at the top. Perform calculations to achieve initial stress equilibrium in this scenario. Excavate the first layer, generating the initial stress field before excavation. Generate models of the cap and pile group within the slope and assign them to convenient groups. Create contact surface elements between the pile group and soil and assign properties to the contact surfaces. Assign properties to the pile group and cap, defining them as the Mohr–Coulomb constitutive model. Apply a vertical static uniformly distributed load on the cap. Run the FLAC3D simulation program, obtaining results under the effect of the strength reduction method. Finally, analyze the results of the FLAC3D simulation and perform visualization processing.

4. Settlement Analysis

4.1. Pile Settlement

Figure 3 illustrates the settlement of a group foundation with piles of equal length and a group foundation with piles of different lengths under a static uniform load of 100 kN. The figure reveals that the largest settlement differences occur at pile 1, pile 6, and pile 9, measuring 2.5 mm, 1 mm, and 1.42 mm, respectively. Specifically, at the location of pile 1, the settlement of the 54 m-long pile is smaller compared to that of the 70 m-long pile.

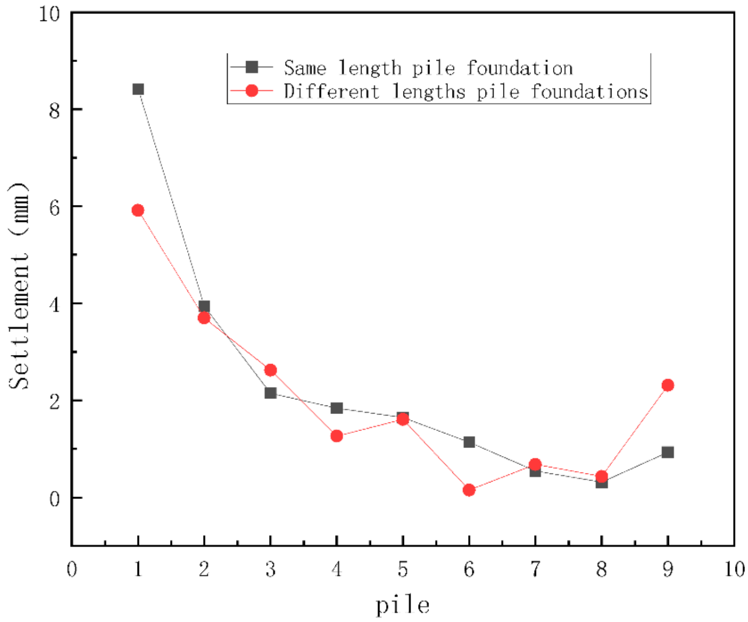

Figure 3. Pile group settlement.

Conversely, at the location of pile 9, where the lengths of the piles are the same, the settlement is smaller in the group foundation with equal-length piles. While the settlement values for other pile positions exhibit a significant degree of overlap, the overall trend suggests that piles with different lengths experience smaller settlements compared to piles with the same length.

The slope and pile arrangement configuration leads to a specific relationship between the cap and the soil. The back half of the cap is in direct contact with the soil, allowing for the transfer of vertical load from above the cap to the slope surface. As a result, this portion of the soil experiences compression. On the other hand, the front half of the cap is not in contact with the soil, and therefore there is no compression occurring in the soil in this area. This difference in soil compression may be the reason for the slightly higher settlement observed in the back row of piles compared to the front row.

4.2. Cap Settlement

Table 2 presents the settlement of the cap in the Y-direction following the application of a 100 kN static uniform axial load, with observation points set at intervals of 5 m. The table highlights that the smallest settlement of the cap occurs near y = 306 m, which corresponds to the middle section without backfill. In the no-backfill section, settlements increase as one moves closer to the edge of the cap. This same trend is observed in the backfill section as well. However, the settlement at the boundary of the backfilled section is more than double compared to the boundary of the no-backfill section.

Table 2. The settlement of pile cap.

Location (m)	276	281	286	291	296	301	306	311	316	321
Settlement (mm)	1040	260	81	30	15	11	6	−25	−322	−1947

Several factors contribute to the settlement of the cap, including the weight of the cap itself, foundation conditions, actual bearing capacity of the pile foundation, negative frictional forces acting on the pile body, lateral deformation of the weak soil layer exerting forward thrust on the pile, and the characteristics of the soil surrounding the cap. The simulated results reveal a significant difference in settlement at both ends of the cap. This discrepancy primarily arises because the soil around the cap was not backfilled and compacted during construction, resulting in minimal binding force on the bearing platform.

Additionally, one side of the cap is backfilled while the other side lacks backfill. The action of the backfill counteracts a substantial portion of the axial load, leading to an upward displacement trend in that particular section of the cap. Simultaneously, the no-backfill section experiences a downward displacement process. As a result, the cap as a whole undergoes forward movement. From this perspective, it is evident that backfilling the cap pit before construction significantly reduces the forward movement of the bridge platform.

5. Displacement Analysis

In Figure 4, the displacements of each pile in the Y-direction are displayed for both the group pile foundation with the same length and the group pile foundation with different lengths. From the graphs, it can be observed that the overall displacement patterns are similar in both cases. The changes in displacement are not significant in the region between 30 m and 65 m from the base of the foundation. However, between 65 m and 80 m, the displacement gradually increases at a slow rate. Beyond approximately 80 m, the displacement of each pile starts to grow rapidly. This indicates that the equivalent sliding surface of the slope is likely located in the range of 80 m to 85 m.

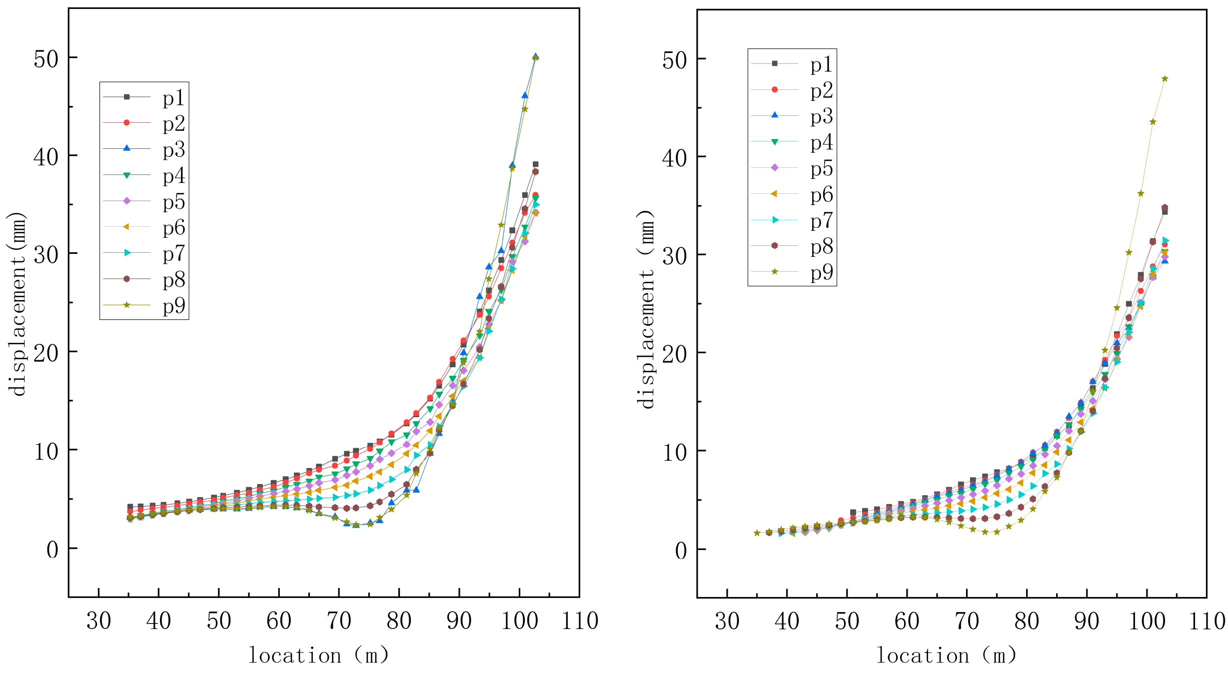

Figure 4. The displacement of different conditions: (**a**) the same length pile; (**b**) the different length pile.

The maximum displacement at the top of the pile is recorded as 48.5 mm, with Pile 9 exhibiting a significantly larger displacement compared to Pile 8. The displacement values at the pile tops, ranging from Pile 1 to Pile 9, display a linear increase. Furthermore, the graph indicates that Pile 9 experiences a negative displacement segment between 65 m and 80 m from the base, followed by a recovery to its original position.

There are two possible explanations for this observation. Firstly, it can be inferred that this section of negative displacement occurs because the outermost pile (Pile 9) is subjected to the largest foundation reaction force within the embedded section. This force surpasses the landslide thrust force, resulting in the generation of negative displacement. Secondly, the finite element simulation process may not have considered characteristics such as slip and detachment between the pile and soil. Consequently, when the soil sinks, it creates a backward pulling force on the pile, contributing to the negative displacement.

6. Bending Moment Analysis

This simulation focused on recording and analyzing the variation of pile bending moments under different static axial loads. The finite element analysis model was incrementally static loaded from 100 kN to 450 kN, with recordings taken at intervals of 50 kN during the loading process. Figure 5a presents the pile bending moments for Pile 1 to Pile 8 under an axial load of 450 kN.

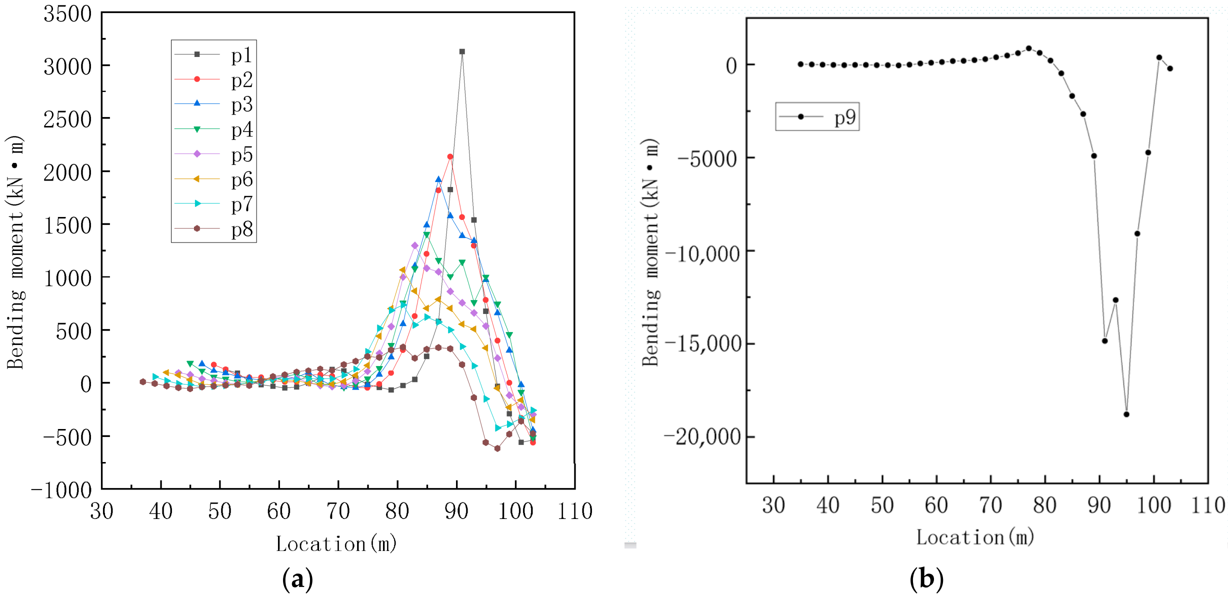

Figure 5. The bending moment under 450 kN load: (**a**) the bending moment of Pile 1 to Pile 8; (**b**) the bending moment of Pile 9.

Due to the significant difference in the bending moments of Pile 9 compared to the other eight piles, the bending moment of Pile 9 is separately displayed in detail in Figure 5b. From these two figures, it is evident that Pile 1 to Pile 8 predominantly experiences positive bending moments with only a small portion of negative bending moments. The variation of the pile body bending moments decreases successively from Pile 1 to Pile 8. The maximum bending moments for Pile 1 to Pile 7 are generally situated in the range of 90 m to 81 m and decrease sequentially. These positions are typically located at the interface between the gravel soil layer and the weakly weathered rock layer. Pile 8, however, has its maximum bending moment located outside the soil layer and exhibits the smallest change in bending moment among the nine piles. On the other hand, the maximum moment point for Pile 9 is at 95 m, precisely at the surface of the gravel soil layer, and there has its maximum bending moment located outside the soil layer and exhibits the smallest change in bending moment among the nine piles. Throughout the loading stages, from 300 kN to 450 kN, the overall state of pile bending moment variation remains relatively unchanged. The maximum bending moment values for each pile continuously decrease as the applied load is reduced, you can see this trend in Figure 6. Notably, the bending moment sudden change point for Pile 9 in the gravel soil layer gradually approaches the maximum bending moment as the load decreases.

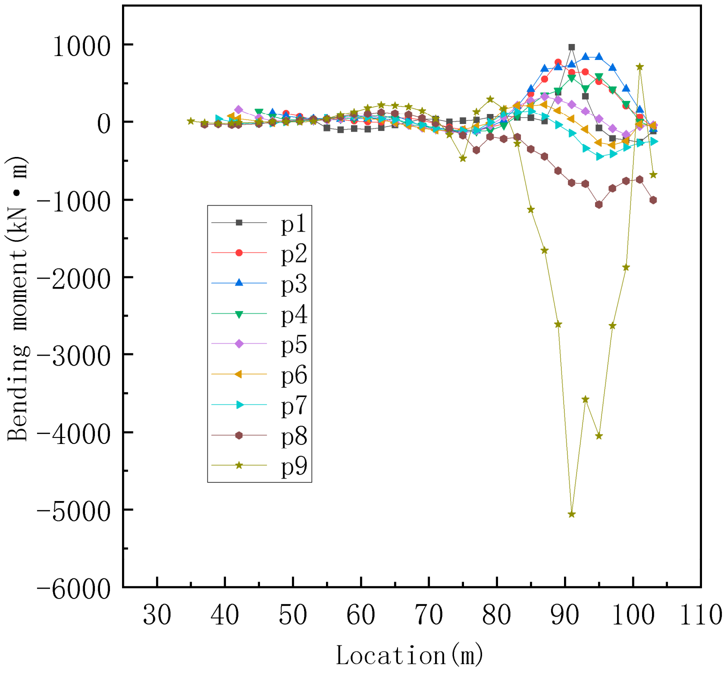

Figure 6. The bending moment under 250 kN load.

From the Figure 7, it can be observed that the maximum bending moment of all piles is negative, and the values of the maximum bending moment are relatively close to each other. The location of the maximum bending moment decreases from the rear pile row to the front pile row. Specifically, the maximum bending moment occurs in the vicinity of the junction between the gravel soil layer and the weakly weathered rock layer, which is where each pile is located.

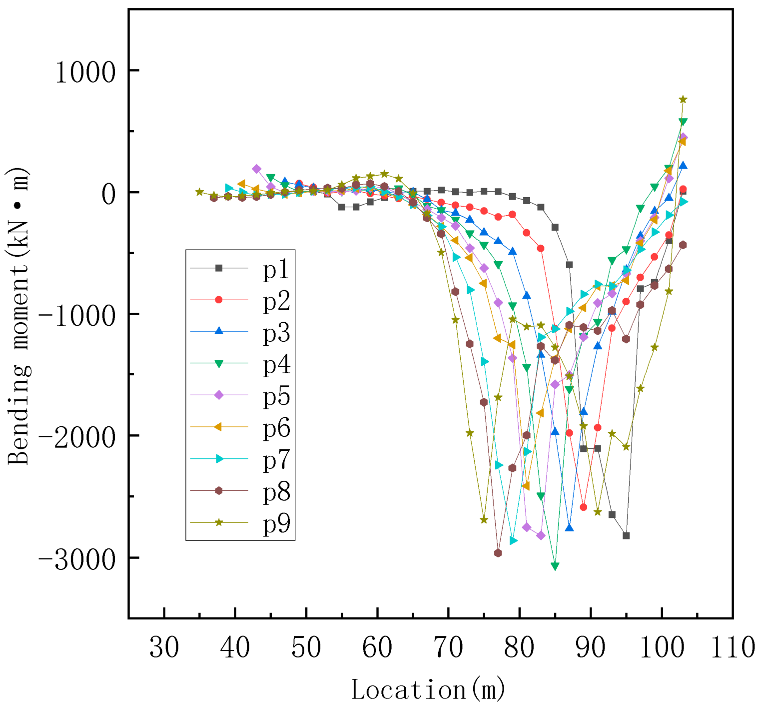

Figure 7. The bending moment under 150 kN load.

7. Plastic Zone and Factor of Safety

As this model adopts the Mohr–Coulomb constitutive model, it adheres to the shear-tension damage criterion. In this context, the term "shear" represents the shear failure element, and "tension" represents the tension failure element. The addition of "n" signifies that the element is currently on the yielding surface during the ongoing calculation time step. Conversely, "p" denotes the past state, indicating that the element was previously on the yielding surface but has since exited and entered the elastic range. When examining plastic zones in practical engineering problems, it is crucial to focus on elements in the "now" plastic state, which actively undergo plastic flow. Only elements in the "now" state influence the instability of the model. Therefore, understanding the elements that are currently yielding is essential for analyzing plastic zones in practical engineering scenarios. The penetration of the plastic zone does not necessarily indicate destruction. Instead, it signifies the extent to which the plastic development of the rock layer has occurred, leading to overall failure and the appearance of multiple plastic zones. The slope's destructive process involves the gradual development of plastic zones, ultimately culminating in overall failure. Therefore, the penetration of the plastic zone is often used as a criterion for assessing slope instability.

From Figure 8, it can be observed that only the uppermost layer of gravel soil exhibits a continuous series of elements in the "now" plastic state. However, under the influence of the rear pile row, this continuity is disrupted. This indicates that the slope in this soil layer is in a stable state due to the reinforcing effect of the group piles.

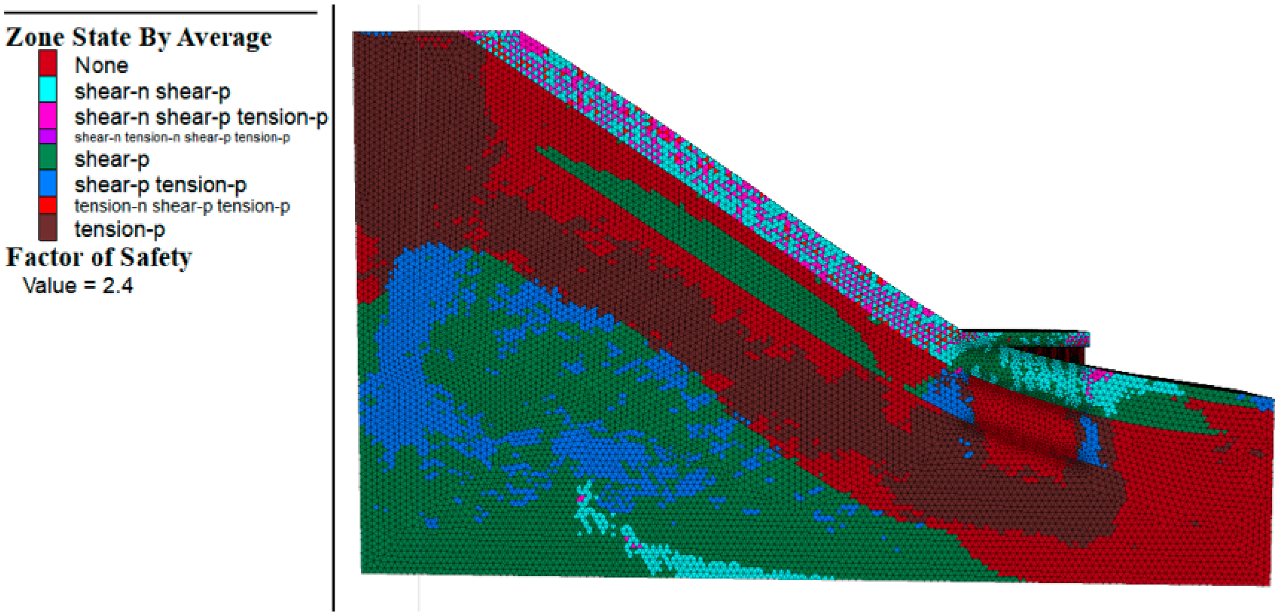

Figure 8. The plastic zone and factor of safety in FLAC3D.

The Factor of Safety (FOS) is another indicator used to assess slope stability, FLAC3D can use the strength reduction method to obtain the factor of safety. In the strength reduction method, the factor of safety for slope stability is defined as the extent to which the shear strength of rock or soil is reduced when the slope is just at the critical failure state. Specifically, the safety factor is defined as the ratio of the actual shear strength of the rock or soil to the reduced shear strength at the critical failure state. Equation (1) can be used to express this.

$$\begin{aligned} c_F &= \frac{c}{F_{trial}} \\ \phi_F &= \tan^{-1}\left(\frac{\tan\phi}{F_{trial}}\right) \end{aligned} \quad (1)$$

The above formula is used to adjust the strength indicators c and ϕ (in this formula, c_F is the adhesive force after reduction, ϕ_F is the friction Angle after reduction, and F_{trial}

is the reduction coefficient). Then, numerical analysis is performed on the slope stability. By continuously increasing the reduction factor, the analysis is repeated until reaching the critical failure state. The reduction factor obtained at this point is the factor of safety.

The output results file from FLAC3D provides the FOS of the model. According to the graph, the FOS is calculated as 2.4. Based on the relevant literature, a slope's FOS should be greater than 1, indicating stability. Thus, the model's calculation results suggest a stable condition. Additionally, the simulation also recorded the FOS under uniformly distributed axial loads ranging from 100 kN to 450 kN, with detailed data available in Table 3.

Table 3. The factor of safety under different loads.

Load (kN)	100	150	200	250	300	350	400	450
Factor of safety	2.4	2.32	2.09	1.78	1.46	1.27	1.14	1.06

From the table, it is clear that as the load increases, the Factor of Safety (FOS) decreases. When the load reaches 450 kN, the FOS is recorded as 1.06. This indicates that the slope's stability is at a critical point. Consequently, if the uniformly distributed axial load exceeds 450 kN, the foundation will become unstable due to the excessively large load.

8. Conclusions

By utilizing numerical simulation methods and considering the engineering reality and geological conditions of large bridges, the bearing capacity characteristics of group pile foundations with different pile lengths were studied, leading to the following conclusions:

Finite element models were established to simulate static load tests on pile foundations with varying pile lengths. Analysis of the vertical load-bearing characteristics of a single pile revealed displacement and settlement curves that align with the load transfer mechanism between the pile and soil. Comparison with a group pile foundation model consisting of piles of the same length demonstrated that the displacement curves were largely similar. This suggests that group pile foundations with different pile lengths and those with the same length exhibit comparable bearing performance. The modeling approach and selected parameters can serve as a reference for similar engineering projects.

Under the axial uniform load, settlement at the pile base varies depending on the location. The middle pile row experiences minimal settlement, while the rear pile row undergoes greater settlement compared to the front pile row. Uneven settlement of the cap is observed, particularly in areas without backfilled soil. In contrast, the cap in the backfilled soil region tends to move upward. To prevent cap tilting, it is recommended to fill the entire bottom area of the cap with soil.

Analysis of the pile group indicates that the location of the maximum bending moment of the pile body is in the region of the gravel soil layer. With small loads, the maximum bending moment is distributed along the soil layer interface. As the load gradually increases, the bending moment direction of the pile body gradually changes, and the maximum bending moment location of the front pile row gradually shifts to the surface of the gravel soil layer.

The distribution revealed by the finite element numerical simulation software of the entire plastic zone confirms that the presence of a group pile foundation disrupts the continuous state of the plastic zone in the uppermost soil layer. This interruption contributes to the stabilization of the upper slope. The factor of safety provides a quantitative method for evaluating the stability of slopes. By comparing the resisting force against sliding to the driving force causing sliding, a numerical value is obtained to assess the stability of the slope under specific conditions. A higher factor of safety implies that the slope's resistance to sliding is relatively greater than the external driving forces. Therefore, when facing external loads or other unfavorable factors, the slope is more likely to remain stable, avoiding sliding or collapse. The obtained Factor of Safety (FOS) of 2.4 further indicates the overall stability of the slope. However, as the load increases, the FOS continues to decrease.

In summary, this study provides insights into the bearing performance of group pile foundations with different pile lengths under vertical loads using finite element numerical simulation methods. The conclusions drawn from this analysis can serve as a reference for related engineering design, yielding cost savings and significant economic benefits while ensuring safety.

Author Contributions: Conceptualization, C.Z.; methodology, C.Z.; software, C.Z., Z.C. and J.Z.; formal analysis, Z.C.; investigation, C.Z.; writing—original draft preparation, C.Z.; writing—review and editing, J.Z.; supervision, C.Z. All authors have read and agreed to the published version of the manuscript.

Funding: This study was financially supported by the National Natural Science Foundation of China (grant number 52208340), the Project of Outstanding Young and Middle-aged Scientific and Technological Innovation Team in Hubei Universities and Colleges (grant number T2022010), and the Doctoral Start-up Fund of Hubei University of Technology (grant number BSQD2020051).

Institutional Review Board Statement: Not applicable.

Informed Consent Statement: Not applicable.

Data Availability Statement: Some or all of the data, models, or code that support the findings of this study are available from the corresponding author upon reasonable request.

Acknowledgments: The authors would like to thank Weiqi Mao and Jinhui Chen for their invaluable contributions to project management and the validation of the results.

Conflicts of Interest: The authors declare no conflict of interest.

Appendix A

FLAC3D	https://www.itasca.fr/en/software/flac3d (accessed on 16 July 2023)
Rhino	https://www.rhino3d.com/ (accessed on 12 June 2023)
hypermesh	https://altair.com/hypermesh (accessed on 7 July 2023)

References

1. De Sanctis, L.; Di Laora, R.; Garala, T.K.; Madabhushi, S.P.G.; Viggiani, G.M.B.; Fargnoli, P. Centrifuge modelling of the behaviour of pile groups under vertical eccentric load. *Soils Found.* **2021**, *61*, 465–479. [CrossRef]
2. Di Laora, R.; de Sanctis, L.; Aversa, S. Bearing capacity of pile groups under vertical eccentric load. *Acta Geotech.* **2019**, *14*, 193–205. [CrossRef]
3. Palammal, J.S.; Senthilkumar, P.K. Behavioural analysis of vertical and batter pile groups under vertical and lateral loading in sand. *Arab. J. Geosci.* **2018**, *11*, 1–7. [CrossRef]
4. Zhang, X.-L.; Xue, J.-Y.; Han, Y.; Chen, S.-L. Model test study on horizontal bearing behavior of pile under existing vertical load. *Soil Dyn. Earthq. Eng.* **2021**, *147*, 106820. [CrossRef]
5. Zhou, L.; Barbato, M.; Ye, A. Experimental Investigation of Postearthquake Vertical Load-Carrying Capacity of Scoured Reinforced Concrete Pile Group Bridge Foundations. *J. Bridge Eng.* **2021**, *26*, 04021091. [CrossRef]
6. Bharathi, M.; Dubey, R.N.; Shukla, S.K. Experimental investigation of vertical and batter pile groups subjected to dynamic loads. *Soil Dyn. Earthq. Eng.* **2019**, *116*, 107–119. [CrossRef]
7. Sheil, B.B.; McCabe, B.A.; Comodromos, E.M.; Lehane, B.M. Pile groups under axial loading: An appraisal of simplified non-linear prediction models. *Geotechnique* **2019**, *69*, 565–579. [CrossRef]
8. Carbonari, S.; Morici, M.; Dezi, F.; Gara, F.; Leoni, G. Soil-structure interaction effects in single bridge piers founded on inclined pile groups. *Soil Dyn. Earthq. Eng.* **2017**, *92*, 52–67. [CrossRef]
9. Bian, X.-Y.; Zheng, J.-J.; Zhang, R.-J.; Xu, Z.-J. Reliability analysis for Serviceability Limit State of pile groups foundation. *Ksce J. Civ. Eng.* **2018**, *22*, 54–61. [CrossRef]
10. Zhang, Y.; Chen, X.; Zhang, X.; Ding, M.; Wang, Y.; Liu, Z. Nonlinear response of the pile group foundation for lateral loads using pushover analysis. *Earthq. Struct.* **2020**, *19*, 273–286. [CrossRef]
11. Chaikla, K.; Thongmunee, S.; Jitsangiam, P.; Chakkaeo, K. Behaviors of Inclined Single Piles and Pile Groups Subjected to Vertical and Horizontal Loads Based on Physical Model Tests in Sand. *Ksce J. Civ. Eng.* **2023**, *27*, 2813–2821. [CrossRef]
12. Liang, F.; Jia, Y.; Xie, W.; Sun, L.; Chen, H. Transverse response of pile group foundations supporting a long-span cable-stayed bridge under uniform and nonuniform excitation. *Soil Dyn. Earthq. Eng.* **2019**, *121*, 57–74. [CrossRef]
13. Chen, Z.; Wang, B.; Gao, X.; Yan, H. Response of Bridge Foundation with Drainage Structure in the Liquefied Inclined Site under Sinusoidal Waves. *Appl. Sci.* **2023**, *13*, 1009. [CrossRef]

14. Fiorentino, G.; Cengiz, C.; De Luca, F.; Mylonakis, G.; Karamitros, D.; Dietz, M.; Dihoru, L.; Lavorato, D.; Briseghella, B.; Isakovic, T.; et al. Integral abutment bridges: Investigation of seismic soil-structure interaction effects by shaking table testing. *Earthq. Eng. Struct. Dyn.* **2021**, *50*, 1517–1538. [CrossRef]
15. Sharafkhah, M.; Shooshpasha, I. Physical modeling of behaviors of cast-in-place concrete piled raft compared to free-standing pile group in sand. *J. Rock Mech. Geotech. Eng.* **2018**, *10*, 703–716. [CrossRef]
16. Ukritchon, B.; Faustino, J.C.; Keawsawasvong, S. Numerical investigations of pile load distribution in pile group foundation subjected to vertical load and large moment. *Geomech. Eng.* **2016**, *10*, 577–598. [CrossRef]
17. Kong, D.; Deng, M.; Li, Y. Numerical Simulation of Seismic Soil-Pile Interaction in Liquefying Ground. *IEEE Access* **2020**, *8*, 195–204. [CrossRef]
18. Qu, L.; Ding, X.; Kouroussis, G.; Zheng, C. Dynamic interaction of soil and end-bearing piles in sloping ground: Numerical simulation and analytical solution. *Comput. Geotech.* **2021**, *134*, 103917. [CrossRef]
19. Kahyaoglu, M.R.; Imancli, G.; Onal, O.; Kayalar, A.S. Numerical analyses of piles subjected to lateral soil movement. *Ksce J. Civ. Eng.* **2012**, *16*, 562–570. [CrossRef]
20. Lian, J.; Lu, W.; Dong, X.; Yang, X.; Yan, X. Numerical evaluation of a new hybrid bucket-group pile foundation for offshore wind turbines. *Ships Offshore Struct.* **2023**, *18*, 22–31. [CrossRef]
21. Kavvadas, M.; Amorosi, A. A constitutive model for structured soils. *Géotechnique* **2000**, *50*, 263–273. [CrossRef]
22. Savvides, A.A.; Papadrakakis, M. A computational study on the uncertainty quantification of failure of clays with a modified Cam-Clay yield criterion. *SN Appl. Sci.* **2021**, *3*, 659. [CrossRef]